

Structures of Gas Phase Oligomeric Gold–Oxygen–Hydrogen Negative Ions Formed by Cesium Ion Bombardment of Vapor-Deposited Gold Surfaces

Gerard Bolbach,^{†,‡} Dennis E. Main,^{†,§} Kenneth G. Standing,[†] and John B. Westmore*^{||}

Departments of Physics and Chemistry, University of Manitoba, Winnipeg, Manitoba R3T 2N2, Canada

Received May 27, 1993[⊗]

Time-of-flight mass spectrometry has been used to examine positive and negative ions desorbed by keV cesium ion bombardment, in high vacuum, of gold surfaces prepared by vapor deposition of gold onto a silver or glass substrate at an ambient pressure of ~ 1 Pa. Many negative ions containing gold, oxygen, and hydrogen were detected; the only positive ion observed, but in small amounts, was Au^+ . The most abundant of the negative ions were Au^- , AuO_2H_n^- ($n = 1-6$), AuO_3H_n^- ($n = 2-4, 6$), $\text{Au}_2\text{O}_4\text{H}_n^-$ ($n = 2-8, 10$), $\text{Au}_2\text{O}_5\text{H}_n^-$ ($n = 3-9, 11$), $\text{Au}_3\text{O}_6\text{H}_n^-$ ($n = 3-8, 10$), $\text{Au}_3\text{O}_7\text{H}_n^-$ ($n = 6-9, 11$), and several more oligomeric ions with a higher gold content. The relative peak height variations for ions belonging to the $\text{Au}_x\text{O}_{2x}\text{H}_y^-$ and $\text{Au}_x\text{O}_{2x+1}\text{H}_z^-$ series ($x = 2$ or 3) exhibited strikingly similar patterns for a given value of x , with an m/z difference of 17 between corresponding parts of the two patterns. Even- and odd-electron compositions are of approximately equal prominence. To account for the abrupt ends of the sequences, the negative ion compositions are rationalized by structures in which the valence shell electron count for gold is ≤ 18 . Some proposals for the 18-electron structures are made. These structures are similar to, but also show differences from, known structures of neutral gold fluorides.

Introduction

Gold surfaces have often been used as supports or backings for thin layers of solid samples to be studied by secondary ion mass spectrometry (SIMS). We have observed that a gold surface formed by vapor deposition yields a multitude of oligomeric gold–oxygen–hydrogen negative ions on bombardment by Cs^+ ions. Since we could not find a precedent for this observation, we report some details of our findings here. The results are of interest both from practical and theoretical viewpoints. In practice, one should be aware of possible background ions that can arise when gold surfaces are used as a backing for samples to be analyzed by SIMS. The theoretical interest lies (i) in clarifying the nature of the gold surface and (ii) in using the observed compositions of the gold-containing negative ions to deduce some of their structures from principles of chemical bonding and to relate them to the known, mainly condensed phase, chemistry of gold.¹⁻³ It is principally to the latter topic that this paper is addressed. We present the results here because, in addition to the discussion of the structures, there are some features of the stoichiometries that can be observed for *isolated* species that are not possible in the condensed phase. We believe that these features will be of interest to inorganic chemists and hope that our proposals will stimulate further investigation of the bonding and structure in these, and related, inorganic species.

Experimental Section

Sample Preparation. A silver foil or glass disk, mounted about 4 cm from a tungsten hairpin filament supporting a small bead of gold, was placed inside a simple bell jar apparatus, which was then evacuated with a sorption pump. After the apparatus was pumped for about 30 min, the tungsten filament was heated to sublime a gold film ~ 500 Å thick (about 160 monolayers) onto the silver or glass substrate. This thickness should ensure complete coverage of the substrate, and in fact, when a silver substrate was used, silver-containing ions were not detected in any positive or negative secondary ion mass spectrum. Although the apparatus lacked a vacuum gauge, we estimate that the ambient pressure during sublimation was ~ 1 Pa (0.01 Torr).

Mass Spectrometry. We used a linear time-of-flight (TOF) mass spectrometer (Manitoba TOF1),^{4,5} fitted with a pulsed thermionic cesium primary ion gun⁶ run at 18 kV, and operating at a background pressure $\leq 10^{-5}$ Pa (10^{-7} Torr), to study ions desorbed from the gold surfaces. The primary Cs^+ ions passed through a high transmission grounded grid before striking the target gold surface. Because the target was at ± 5 kV, the primary ions struck the surface with energies of ~ 13 or ~ 23 keV for positive/negative secondary ion studies, respectively. The primary ion pulses, 3 ns wide at half-maximum, repeated at a frequency of 4 kHz, struck the gold surface at an angle of $\sim 20^\circ$ to the normal, with an average primary ion current of 0.1–1 pA (6×10^5 – 6×10^6 ions s^{-1} , i.e. 150–1500 ions pulse⁻¹). Thus, for the longest irradiation time of 30 min, we estimate the total radiation dose on the 1 mm² surface exposed to the primary ion beam to be 10^9 – 10^{10} Cs^+ ions. Since we estimate this surface area to contain about 10^{13} gold atoms, we have a *maximum* dose of 1 incident Cs^+ ion/1000 surface gold atoms. Consequently, radiation damage to the surface should be insignificant, an expectation supported by the lack of change in the spectrum up to the maximum 30 min irradiation time. The secondary ions, accelerated to 5 keV energy by the grid, which was ~ 2 mm from the gold surface, passed through a linear field-free region to a microchannel plate electron multiplier detector located at the far end of the flight tube, 1.55 m from the acceleration grid. The detector

[†] Department of Physics.

[‡] On leave from Institut Curie, 11 rue Pierre et Marie Curie, 75231 Paris Cedex 05, France.

[§] Present Address: Atomic Energy of Canada Ltd., Corporate Office, 275 Slater Street, Ottawa, Ontario K1A 0S4, Canada.

^{||} Department of Chemistry.

[⊗] Abstract published in *Advance ACS Abstracts*, October 15, 1994.

- (1) Puddephatt, R. J. *The Chemistry of Gold*; Elsevier: Amsterdam, The Netherlands, 1978.
- (2) Cotton, F. A.; Wilkinson, G. *Advanced Inorganic Chemistry*, 5th ed.; Wiley-Interscience: New York, 1988.
- (3) Puddephatt, R. J. In *Comprehensive Coordination Chemistry*; Wilkinson, G., Ed.; Pergamon Press: Oxford, U. K., 1987; Vol. 5, pp 861–923.

(4) Chait, B. T.; Standing, K. G. *Int. J. Mass Spectrom. Ion Phys.* **1981**, *40*, 185–193.

(5) Standing, K. G.; Beavis, R.; Ens, W.; Schueler, B. *Int. J. Mass Spectrom. Ion Phys.* **1983**, *53*, 125–134.

(6) Allison, S. K.; Kamegai, M. *Rev. Sci. Instrum.* **1961**, *32*, 1090–1092.

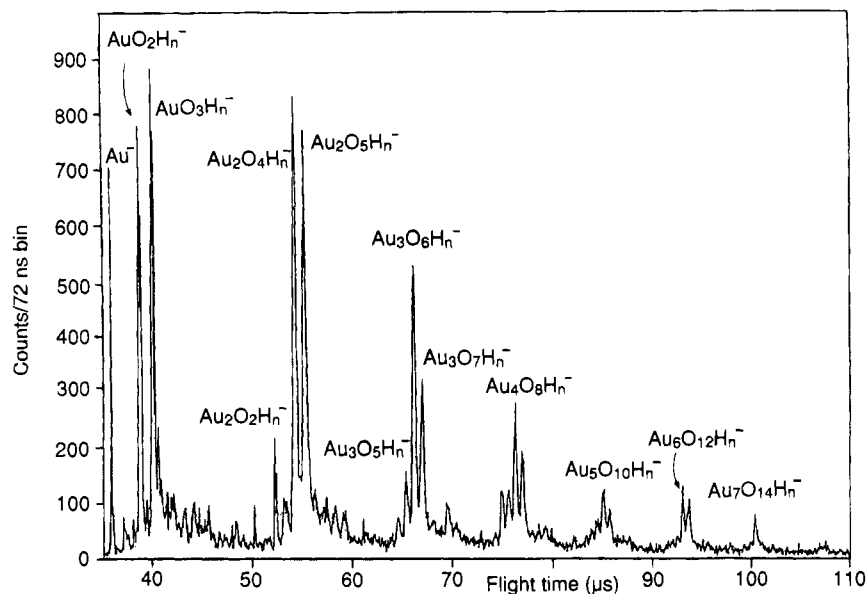


Figure 1. Complete negative ion time-of-flight mass spectrum produced by cesium ion bombardment of a vapor-deposited gold film.

output was processed by a data acquisition system based on a LeCroy Model 4208 time-to-digital converter (TDC) and a DEC LSI 11/23 computer.⁷

Results and Discussion

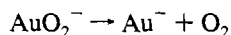
Positive Ion Spectrum. A small peak at m/z 197 was assigned to Au^+ . The spectrum was very clean above m/z 197 indicating that, beyond this value, gold surfaces are excellent sample backings for positive SIMS. At lower m/z values the usual multitude of peaks from small amounts of adsorbed organic molecules, and a sizable peak at m/z 149, assigned to the ubiquitous fragment ion from di-*n*-butyl phthalate plasticizer, were present.

Negative Ion Spectrum. The complete negative ion spectrum (Figure 1) shows, in addition to Au^- , peaks assignable to ions containing one or more gold atoms combined with varying numbers of oxygen and hydrogen atoms. (We have also detected these ions from gold surfaces deposited at an ambient pressure of 10^{-3} – 10^{-4} Pa. Their abundances are much smaller than those observed from the present surface, deposited at ~ 1 Pa, but the groups containing one gold atom are generally easily detected.) In general, many factors, including rates of formation and decomposition, influence the abundances of detected ions but, to be recorded as a sharp peak at a discrete flight time, the ions must be formed promptly, near the sample surface, and must survive the acceleration period (about 10^{-7} s).⁸ Furthermore, should an ion decompose during field-free flight, its daughters (ion and neutral) continue toward the detector at the same velocity as the parent (except for a small velocity component introduced by kinetic energy release during decomposition). Although the daughter particles reach the detector at approximately the same time as nondecomposing parent ions, such KE release would lead to broadening at the base of the recorded peaks. Failure to observe broadening at the bases of the peaks implies that the negative ions do not undergo metastable decay and are, therefore, stable on a time scale of several tens of μs , and we have assumed that the abundances of detected negative ions roughly correspond to the relative

numbers of them leaving the surface. We here discuss some structural features of the desorbed species that are likely to be of major importance in determining their stability. These species will be described in order of increasing complexity.

Monogold-Containing Negative Ions. In the expanded spectrum (Figure 2) the negative ions Au^- , AuO_2H_n^- ($n = 1$ – 6), and AuO_3H_n^- ($n = 2$ – $4, 6$) are prominent. AuO_3H^- and AuO_3H_5^- are also observed, but in low yields. In contrast to the mass spectra of organic compounds, both even- and odd-electron ions are prominent, no doubt owing to the presence of the transition metal.

The high abundance of Au^- is consistent with the relatively high electron affinity (2.309 eV⁹) of the gold atom. On the other hand, ions such as AuH^- , AuO^- , AuOH^- , AuO_2^- , and AuO_3^- are conspicuously absent. Neutral AuH and AuO are known species (the bond dissociation energies, D , are as follows: $D(\text{Au}-\text{H}) = 3.22$; $D(\text{Au}-\text{O}) = 2.33$ (eV/molecule)¹⁰). The species AuH^- and AuOH^- are probably unstable with respect to electron loss for, in either case, the extra electron can only be placed in an antibonding orbital or a higher energy nonbonding gold p orbital and would, even if bound, be only weakly so. On the other hand, any reasonable bonding scheme for AuO^- and AuO_2^- (as O^-AuO^-) would dictate that all electrons are bound. Thus, we expect AuO^- to be intrinsically stable and its absence may mean that, in the presence of adsorbed water, OH and H are the dominant species bound to the surface. The absences of AuO_2^- and AuO_3^- can be similarly explained. However, an alternative explanation for the absence of AuO_2^- can be offered, for it might be unstable with respect to the dissociation:



$$D(\text{Au}^- - \text{O}_2) = A(\text{AuO}_2) + D(\text{Au}-\text{O}_2) - A(\text{Au})$$

Here A represents electron affinity. Our failure to locate thermochemical data for AuO_2 suggests that it might be unstable,

(7) Ens, W.; Beavis, R.; Bolbach, G.; Main, D.; Schueler, B.; Standing, K. G. *Nucl. Instrum. Meth.* **1986**, *A245*, 146–154.

(8) Lafortune, F.; Ens, W.; Hruska, F. E.; Sadana, K. L.; Standing, K. G.; Westmore, J. B. *Int. J. Mass Spectrom. Ion Processes* **1987**, *78*, 179–194.

(9) Hotop, H.; Lineberger, W. C. *J. Phys. Chem. Ref. Data* **1985**, *14*, 731–750. Cited in: *NIST Negative Ion Energetics Database, NIST Standard Reference Database 19B*, National Institutes of Science and Technology: Gaithersburg, MD, 1990. Compiled by J. E. Bartmess.

(10) Huber, K. P.; Herzberg, G. *Molecular Spectra and Molecular Structure. IV. Constants of Diatomic Molecules*. Van Nostrand Reinhold Co.: New York, 1979.

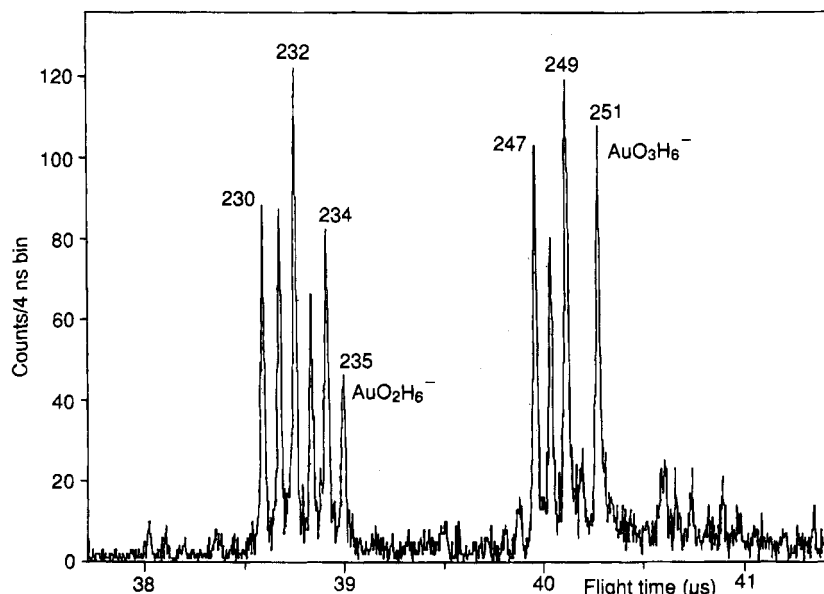
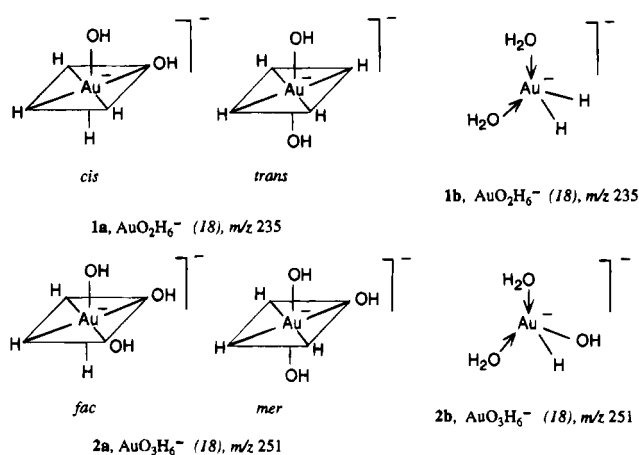


Figure 2. Expanded section of Figure 1 showing detail of peaks for monogold-containing negative ions.

i.e. $D(\text{Au}-\text{O}_2)$ is very small. If this is so, then $D(\text{Au}^--\text{O}_2)$ would be small unless $A(\text{AuO}_2)$ is significantly greater than 2.309 eV. If $A(\text{AuO}_2)$ is <2.3 eV, then Au^--O_2 would be unstable with respect to dissociation.

To rationalize the range of gold-containing negative ion compositions observed we must be aware of the number of electrons in the valence shell of the metal. In the subsequent discussion, for purposes of electron counting we have adopted the method used in a leading text² by regarding hydrogen and hydroxyl radicals as neutral one-electron donor ligands and their bonds to gold as covalent bonds, represented in canonical structures by simple solid lines. Water is regarded as a two-electron donor ligand, with the ligand→metal bond represented by an arrow. Gold(0) retains 11 electrons in its valence shell. (This procedure is simpler than an alternative, popular, electron-counting method¹¹ that regards hydride and hydroxide ions as two-electron donor ligands, with a corresponding adjustment of the metal oxidation state. Of course, either of these electron-counting procedures leads to the same number of metal valence shell electrons but they yield different formal oxidation states.)

The number of hydrogens observed in the di- and trioxoxygen-containing negative ions reaches a maximum at six hydrogens, with no indication of species with a higher hydrogen content. The 18-electron rule^{2,11} (normally applied to nonclassical transition metal complexes), which states, in part, that the number of valence shell electrons of a transition metal may attain a maximum value of 18, explains why more than six hydrogens are not incorporated. Thus, if the negative charge is centralized on gold (i.e. the extra electron is formally placed in a gold orbital), then the number of gold valence shell electrons is given by $(12 + n)$ for n hydrogens in any combination of water, hydroxy, or hydrogen ligands, irrespective of the negative ion geometry, and therefore equals 18 for six hydrogens. The latter situation is illustrated for octahedral (**1a, 2a**) or tetrahedral (**1b, 2b**) structures and would also hold true for three-coordinate $[\text{Au}(\text{H}_2\text{O})_3]^-$. (In these, and subsequent structures, we show the number of gold valence shell electrons in parentheses after the ion formula.) We prefer to assign octahedral structures to the AuO_2H_6^- and AuO_3H_6^- species because tetrahedral (and also three-coordinate) structures require the participation of



gold–water bonds; these would be very weak because they involve a neutral ligand and low-valent gold. On the other hand, in an octahedral structure the more polar gold–hydroxy bonds should be considerably stronger. Henceforth, we assume that a gold–hydroxy plus a (well-known) gold–hydrogen bond will always be formed in preference to a gold–water bond, a practice that leads to a consistent interpretation of the results.

We deliberately avoid discussion of formal oxidation states of gold owing to incongruities associated with conventional ideas of gold chemistry, such as the following in which the hydrogen ligand is regarded as hydride. The formal oxidation states of gold in **1a** and **2a** are then both +5. However, a gold(V) hydride is unlikely because hydride is strongly reducing. On the other hand, the oxidation state of gold would be +1 in both **1b** and **2b**, and thus a two-coordinate, linear, rather than a four-coordinate, tetrahedral, structure is to be expected.

Negative ions with fewer than six hydrogens and, therefore, fewer than 18 gold valence electrons are abundant. For the most part, their structures are easily explained by removing the appropriate number of gold–hydrogen bonds from **1a** and **2a**. (The exceptions are OAuOH^- and $\text{OAu}(\text{OH})_2^-$, for which oxygen–hydrogen bonds must also be formally removed in their formation from **1a** and **2a**, respectively.) As stated, for these ions there are fewer than 18 valence electrons for gold, but of course, in the EI (electron ionization) and LSI (liquid secondary ionization) mass spectra of transition metal complexes, ion

(11) Collman, J. P.; Hegedus, L. S.; Norton, J. R., Finke, R. G. *Principles and Applications of Organotransition Metal Chemistry*; University Science Books: Mill Valley, CA, 1987.

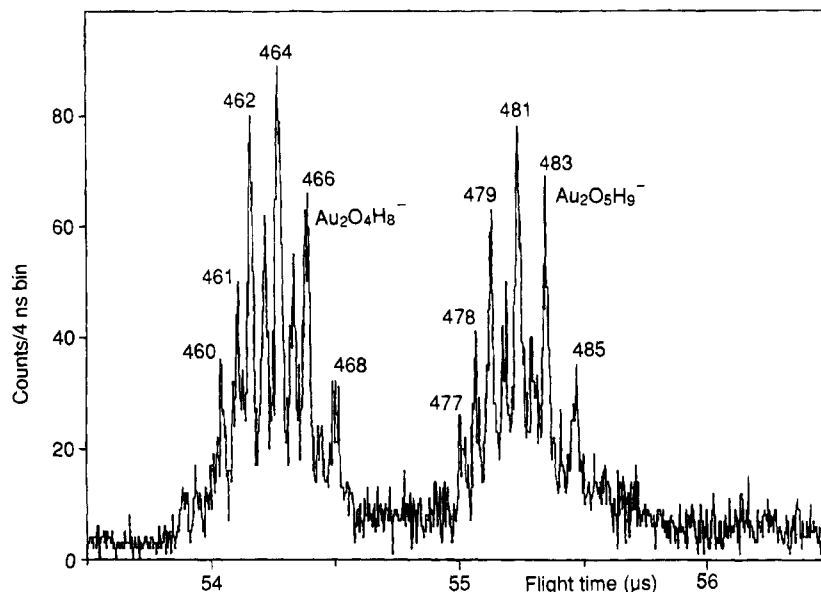


Figure 3. Expanded section of Figure 1 showing detail of peaks for digold-containing negative ions.

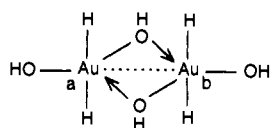
species where the metal has an incomplete d shell are well-known.

The relatively low abundance of $\text{Au}_2\text{O}_3\text{H}_5^-$ (m/z 250) compared to the high abundance of $\text{Au}_2\text{O}_2\text{H}_5^-$ (m/z 234) is noteworthy because gold has 17 valence shell electrons in both species. This curious observation has analogues for ion sequences containing two and three gold atoms.

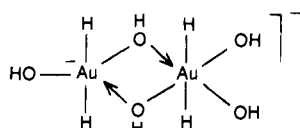
Digold-Containing Negative Ions. The expanded spectrum (Figure 3) shows $\text{Au}_2\text{O}_4\text{H}_n^-$ ($n = 2-8, 10$) and $\text{Au}_2\text{O}_5\text{H}_n^-$ ($n = 3-9, 11$) as the most abundant negative ions. The high/low peak height patterns are similar for the two ion sequences, including the curiously small peak heights for $n = 9$ and $n = 10$, respectively, for the former and latter sequences. Notably small are peaks for negative ions containing fewer than four oxygen atoms. Also present, but of low abundance, are negative ions containing 6–9 oxygen atoms.

The detection of Au_2^- is uncertain. Although Au_2 is a stable molecule ($D(\text{Au}-\text{Au}) = 2.30 \text{ eV}^{10}$), an extra electron would be only weakly bound, if bound at all, since it would be placed in an antibonding orbital. The spectrum may show a small peak barely discernible above the background noise at the correct m/z value for Au_2^- , but this observation is inconclusive.

The $\text{Au}_2\text{O}_4\text{H}_n^-$ and $\text{Au}_2\text{O}_5\text{H}_n^-$ groups of peaks each show similar alternations of high/low relative peak heights. The high peaks occur at even n for the first, and at odd n for the second, group. Thus, the even/odd electron character of the high/low ion peaks is reversed. Corresponding parts of the two patterns have a mass difference of 17 u. Ions corresponding to the high peak heights incorporate maxima of eight and nine hydrogens for the first and second groups, respectively. Hypothetically, these ions can be constructed from the credible structure 3 for



3, $\text{Au}_2\text{O}_4\text{H}_8$ (18-18), $M_r = 466$



4, $\text{Au}_2\text{O}_5\text{H}_9^-$ (18-18), m/z 483

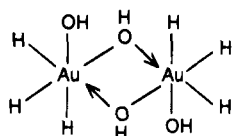
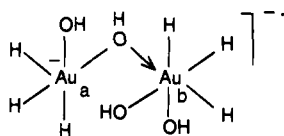
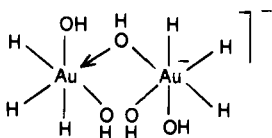
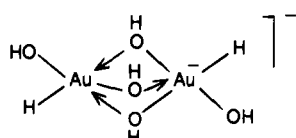
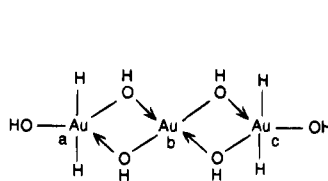
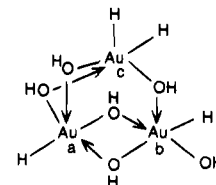
the neutral species $\text{Au}_2\text{O}_4\text{H}_8$. We regard a bridging hydroxy ligand as a three-electron donor so that each gold atom has 17 valence shell electrons if the interaction between the gold atoms is weak (i.e. the overlap between gold d orbitals of appropriate

symmetry is small), or 18 if the interaction is strong enough that metal–metal bonding can be invoked, as shown in 3. The possibility of strong interaction is supported by many examples of gold–gold bonding in electron-deficient organogold compounds.¹² Addition of an electron to 3 produces $\text{Au}_2\text{O}_4\text{H}_8^-$, m/z 466. In the case of weak interaction, this electron can be placed on one gold atom, so that the gold atoms can be assigned 18 and 17 valence shell electrons, respectively. Alternatively, in the case of strong metal–metal interaction in the neutral species, the added electron will be placed in a formally antibonding orbital. However, the effect of doing this would be to increase the gold–gold separation so that the overlap of the d orbitals could be decreased to the point at which the interaction is weak, to give effectively the same situation as before. Thus, violation of the 18-electron rule can be avoided, but which description applies is uncertain. Addition of a hydroxide ion to 3 would produce $\text{Au}_2\text{O}_5\text{H}_9^-$, to which we assign structure 4, in which both gold atoms have an 18-electron valence shell. Compared to this abundant ion, the relatively low abundance of $\text{Au}_2\text{O}_4\text{H}_9^-$, m/z 467, is curious because it only differs from 4 by formal replacement of OH^- by H^+ (i.e. both gold atoms have 18 valence shell electrons).

In addition to these abundant ions there are also minor species incorporating maxima of 10 and 11 hydrogens for tetra- and penta-oxygen-containing negative ions, respectively. As above, a hypothetical construction of $\text{Au}_2\text{O}_4\text{H}_{10}^-$ and $\text{Au}_2\text{O}_5\text{H}_{11}^-$ from $\text{Au}_2\text{O}_4\text{H}_{10}$, 5, by addition of an electron or hydroxide ion can be performed. As structure 5 is written both gold atoms have 18 valence shell electrons. An electron can be added, to produce $\text{Au}_2\text{O}_4\text{H}_{10}^-$, 6, only at the expense of a hydroxide bridge if the 18-electron rule is to be obeyed. In 6, Au_a and Au_b are assigned 17 and 18 electrons, respectively. Alternatively, addition of hydroxide ion to 5 would produce $\text{Au}_2\text{O}_5\text{H}_{11}^-$, 7, in which both gold atoms have 18-electron valence shells.

Only one bridging hydroxide group is possible in structures 6 and 7 if the 18-electron rule is to be obeyed. The resulting decrease in stability may explain why these negative ions are less abundant than the doubly bridged negative ions 3 and 4 and why the relative abundance of $\text{Au}_2\text{O}_4\text{H}_{11}^-$, m/z 469, like 7, would also be singly bridged (its gold atoms are isoelectronic with those in 7 because H^+ replaces a terminal

(12) Reference 3, p 899.

5, $\text{Au}_2\text{O}_4\text{H}_{10}$ (18-18), $M_r = 468$ 6, $\text{Au}_2\text{O}_4\text{H}_{10}^-$ (17-18), m/z 4687, $\text{Au}_2\text{O}_5\text{H}_{11}^-$ (18-18), m/z 4858, $\text{Au}_2\text{O}_5\text{H}_7^-$ (18-18), m/z 4819, $\text{Au}_3\text{O}_6\text{H}_{10}$ (a17-b17-c17), $M_r = 673$ 10, $\text{Au}_3\text{O}_6\text{H}_{10}^-$ (a18-b18-c17), $M_r = 673$

*OH), is also small. It follows that increasing the hydrogen atom content of negative ions is ultimately achieved at the expense of bridging capabilities if the 18-electron rule is to be obeyed. Thus, digold-containing negative ions with more than 11 hydrogens are neither expected nor observed.

On the other hand, as argued for monogold-containing ions, decreasing the hydrogen atom content decreases the number of electrons available for the gold valence shells. It follows from the preceding discussion that this decrease can be partially offset by increasing the number of hydroxy bridges (to a maximum of three). Thus, some of the negative ions containing fewer than eight hydrogen atoms may be triply bridged. For example, structure 8, in which both gold atoms have 18 valence shell electrons, is a possibility for the prominent species $\text{Au}_2\text{O}_5\text{H}_7^-$. (Of course, if increased bridging does not occur, then the gold valence shells do not attain 18 electrons.)

As the hydrogen content of the ions decreases further, even for triply bridged structures the valence electron count for gold becomes <18 , and, as before, the structures of the ions can be explained by formal removal of gold–hydrogen bonds. We assume that at least two bridging groups are retained in the ion structures.

We observe that the 17 u mass difference between the corresponding patterns of the two main groups of peaks implies rather similar roles for the electron and hydroxide ion in the formation of the negative ions, in spite of the reversed odd–even electron character that would result. Since, in each case, the odd electron resides formally in gold-based orbitals, the normal dominating effect of odd–even electron character upon the prominent ions observed in mass spectra becomes less significant.

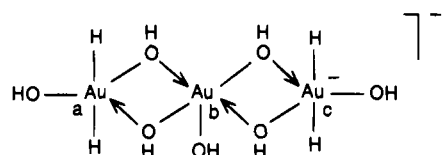
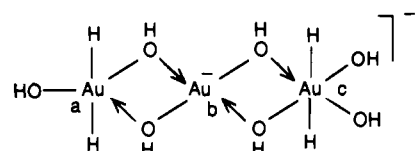
Trigold-Containing Negative Ions. The expanded spectrum (Figure 4) shows $\text{Au}_3\text{O}_6\text{H}_n^-$ ($n = 3-8, 10$) and $\text{Au}_3\text{O}_7\text{H}_n^-$ ($n = 6-9, 11$) as major negative ions. Again, these sequences show alternations of high/low relative peak heights, as well as the curiously small, or absent, peaks corresponding to $n = 9$ and $n = 10$, respectively, for the former and latter sequences. The high peaks occur at even n for the former ion and at odd n for the latter ion. As before, a mass difference of 17 u is observed between corresponding parts of the patterns. Minor species observed are $\text{Au}_3\text{O}_4\text{H}_n^-$ and $\text{Au}_3\text{O}_5\text{H}_n^-$.

We suggest that the abundant ions with the maximum hydrogen content, namely $\text{Au}_3\text{O}_6\text{H}_{10}^-$ and $\text{Au}_3\text{O}_7\text{H}_{11}^-$, can be rationalized by a hypothetical construction starting from neutral $\text{Au}_3\text{O}_6\text{H}_{10}^*$. One possible structure, 9, for this molecule has a chain of gold-containing units. For weak metal–metal interactions, each gold atom has 17 valence shell electrons, and an added electron, formally placed on one of the gold atoms, gives an a17-b18-c17 or a18-b17-c17 gold valence electron count in $\text{Au}_3\text{O}_6\text{H}_{10}^-$. Alternatively, for strong metal–metal interactions, each gold atom can supply a d orbital, of appropriate symmetry, to form three MOs, in which ψ_1 (bonding) contains an electron

pair, ψ_2 (formally nonbonding) contains a single electron, and ψ_3 (antibonding) is unoccupied. (The net overlap of the participating gold d orbitals would be influenced more by the gold–gold separation than by whether the $\text{Au}(\text{O})_2\text{Au}$ unit is planar or slightly folded at the line joining the oxygen atoms.) When the high electron affinity of gold is recalled, the addition of an electron to ψ_2 can be anticipated to occur readily to yield an ion stabilized by delocalization of the charge and with an 18-electron count for each gold atom.

We have also considered the possibility of cyclic neutral trimer precursors for the ions. For $\text{Au}_3\text{O}_6\text{H}_{10}^*$ no more than five bridging groups are possible, structure 10, if the 18-electron rule is to be obeyed. With this procedure two gold atoms have 18, and the third 17, valence electrons. (As shown, gold atom *c* is electron deficient, but any of the three could be regarded as electron deficient by appropriate movements of electrons.) An electron added to the third gold atom of 10 would form $\text{Au}_3\text{O}_6\text{H}_{10}^-$.

Addition of hydroxide ion to 9 yields the species $\text{Au}_3\text{O}_7\text{H}_{11}^-$, to which structures 11 or 12 can be assigned. Addition of hydroxide ion to 10 could occur but only at the expense of decreased bridging.

11, $\text{Au}_3\text{O}_7\text{H}_{11}^-$ (a17-b18-c18), m/z 69012, $\text{Au}_3\text{O}_7\text{H}_{11}^-$ (a17-b18-c18), m/z 690

The ions $\text{Au}_3\text{O}_6\text{H}_{12}^-$ and $\text{Au}_3\text{O}_7\text{H}_{12}^-$, which are permitted for chain structures by the procedures outlined here, are not observed, at least, as major species.

Negative ions containing fewer than 10 hydrogen atoms can often be represented by structures that are consistent with the 18-electron rule if the number of hydroxy bridges is increased, either in chain or cyclic trimers. In the ion compositions for which this does not occur the gold valence shells contain fewer than 18 electrons.

Polygold-Containing Negative Ions. Several more oligomeric ions were observed. The most abundant of these can be described by the following formulas: $\text{Au}_4\text{O}_x\text{H}_y^-$ ($x = 6-9$); $\text{Au}_5\text{O}_x\text{H}_y^-$ ($x = 10-12$); $\text{Au}_6\text{O}_x\text{H}_y^-$ ($x = 12, 13$); $\text{Au}_7\text{O}_x\text{H}_y^-$ ($x = 14$). The groups of peaks were not well enough resolved to determine the relative peak height dependence upon y , and at present, we can only say that the y values range approximately from $x - 4$ to $x + 4$. In each ion, there are about twice as many oxygen as gold atoms, an observation consistent with

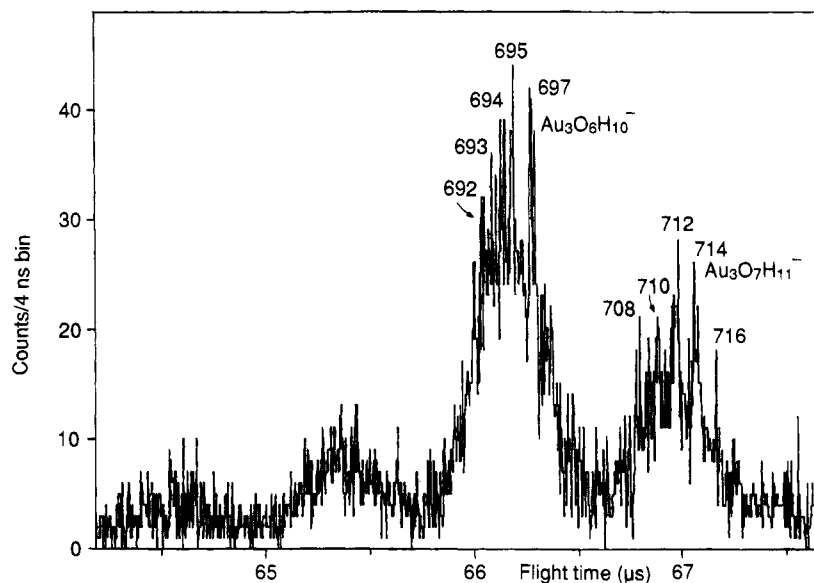
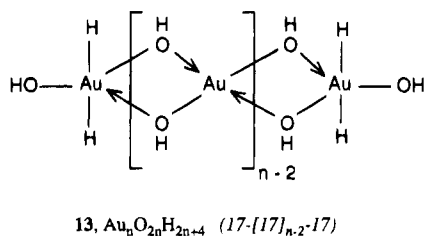


Figure 4. Expanded section of Figure 1 showing detail of peaks for trigold-containing negative ions.

structures in which gold atoms are bridged by two hydroxy groups. For example, on the basis of earlier discussion, we may consider negative ion formation from the neutral molecule $Au_nO_{2n}H_{2n+4}$. In a chain structure, **13**, for weak metal-metal



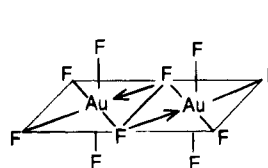
interactions, each gold atom has 17 valence shell electrons. For strong interactions, each gold atom can supply a d orbital of appropriate symmetry to form the same number of MOs. If n is even, all electrons are paired in bonding MOs. If n is odd, one electron, in an approximately nonbonding MO, is unpaired. Thus, for reasons given earlier for formation of the $Au_2O_4H_8^-$ and $Au_3O_6H_{10}^-$ ions, respectively, an electron or hydroxide ion should be readily added to **13**, for either weak or strong metal-metal interactions, for either even or odd n .

Species with higher oxygen content than in **13** can be explained by replacement of hydrogen on terminal gold atoms by hydroxy ligands. This procedure does not change the electron count as far as a gold atom is concerned. If the 18-electron rule is to be observed, an increase in hydrogen content in an anion ultimately decreases the number of hydroxy bridges (with an anticipated decrease in stability and, hence, abundance), while a decrease in hydrogen content may increase the number of hydroxy bridges.

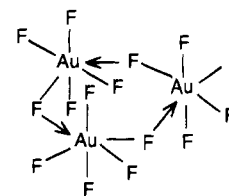
Structures other than chains (e.g. rings, branched chains, sheets, or three-dimensional structures) are conceivable for ions of higher oligomers. These can be rationalized by using arguments similar to those presented earlier for the trimers.

Comparison of Negative Ion Structures with Those of Neutral Gold Fluorides. It is instructive to compare the structures proposed for the negative ions with known structures of gold fluorides because the fluorine atom is isoelectronic with the hydroxy radical and, like a hydrogen atom, can be regarded as a one-electron donor ligand.

Gaseous gold pentafluoride was shown by electron diffraction to consist mostly of dimeric molecules, Au_2F_{10} , though trimeric molecules, Au_3F_{15} , were also present,¹³ an observation supported by mass spectrometry.¹⁴ In the least squares fitting procedure used, D_{2h} and D_{3h} symmetries were assumed for the dimer and trimer, respectively, to yield structures **14** and **15** in which both



14, Au_2F_{10} (18-18)



15, Au_3F_{15} (18-18-18)

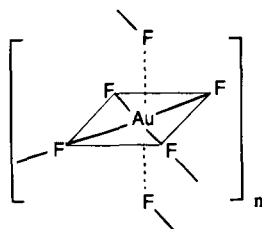
gold atoms are surrounded by six fluorine atoms in distorted octahedral arrangements. Structure **14** may be compared to structures **3** and **4**. The common features of each structure are gold atoms with 18 valence shell electrons and metal atoms doubly bridged by isoelectronic ligands. The abundant ion $Au_2O_5H_9^-$ (structure **4**) is a close analogue of **14**, but $Au_2O_4H_9^-$, also a close analogue, is not abundant (see Figure 3). In structure **15**, where each gold atom again has 18 valence shell electrons, each gold atom is linked by single fluorine bridges to two neighbors. The closest analogous negative ion compositions, $Au_3O_mH_{14}^-$, are not detected. More highly bridged structures **9-12** have been proposed to account for the lower hydrogen contents actually observed.

In the solid state, gold trifluoride (which is diamagnetic, d^8) was shown by X-ray diffraction to be a fluorine-bridged polymer¹⁵ containing square planar AuF_4 units linked by *cis* fluorine bridges (structure **16**). Here the gold atoms have only 16 valence shell electrons; i.e., the structures have not made use of triple fluorine bridging to raise the gold electron counts to their full complements. Instead, each gold atom supplies a

(13) Brunvoll, J.; Ischenko, A. A.; Ivanov, A. A.; Romanov, G. V.; Sokolov, V. B.; Spiridonov, V. P.; Strand, T. G. *Acta Chem. Scand.* **1982**, *A36*, 705-709.

(14) Vasile, M. J.; Richardson, T. J.; Stevie, F. A.; Falconer, W. E. *J. Chem. Soc., Dalton Trans.* **1976**, 351-353.

(15) Einstein, F. W. B.; Rao, P. R.; Trotter, J.; Bartlett, N. *J. Chem. Soc. A* **1967**, 478-492.

16, $(\text{AuF}_3)_n$ $(16)_n$

d orbital for stacking interactions between fluorine and gold atoms perpendicular to the square planes. Although the compositions of the polyatomic negative ions are less precisely known, it is evident that the arguments presented here lead to structures (such as **13**) that are more highly bridged than **16**.

Thus, there are similarities among the proposed negative ion structures and known structures for neutral gold fluorides but also significant differences. These differences may result more from the composition of the gold surface and the way in which the negative ions are formed than from differences in their stabilities. Although much remains unknown about the processes involved in formation of the ions, to explain the 17 u mass difference between ion sequences, it is tempting to suggest that both electrons and hydroxide ions, because they would be among the products of energetic particle bombardment of a hydroxide-covered surface, could be added to neutral gold-containing species as they are desorbed from the surface.

Conclusion

The hydrogen to oxygen ratio in gold-containing ions, when integrated over all negative ions, lies between 1:1 and 2:1, a result that is consistent with a surface layer formed from a mixture of adsorbed water and molecular oxygen (or their derived products). It is possible, even likely, that the negative ion spectrum does not accurately reflect the nature of the gold surface. Nevertheless, these results indicate that gold–oxygen bonds, and probably gold–hydrogen bonds, are present at the gold surface. This important problem has not been addressed in this paper, but many experiments could be performed to investigate the composition and reactivity of the surface by exposing it to varying partial pressures of H_2O , D_2O , or O_2 and later detecting the ions desorbed by energetic particle bombardment.

We have observed that the secondary negative ions studied here do not undergo metastable decay so that this source of information about their structures is not available. While TOF mass spectrometry does not easily lend itself to collisionally assisted dissociation experiments, they could be performed in multiple sector or triple quadrupole mass spectrometers fitted with particle bombardment sources.

Acknowledgment. This work was supported by grants from the U.S. National Institutes of Health (Institute of General Medical Sciences) and from the Natural Sciences and Engineering Research Council of Canada.